

Mechanical aspects of pull-apart basins and push-up swells with applications to the Dead Sea transform

ZE'EV RECHES

Department of Geology, Hebrew University, Jerusalem (Israel)

(Received November 5, 1985; accepted July 2, 1986)

Abstract

Reches, Z., 1987. Mechanical aspects of pull-apart basins and push-up swells with applications to the Dead Sea transform. In: Z. Ben-Avraham (Editor), *Sedimentary Basins within the Dead Sea and Other Rift Zones*. *Tectonophysics*, 141: 75–88.

Pull-apart basins and push-up swells are common features at steps along strike-slip faults. The structure of these features is examined here for two types of rheology: perfect brittle and perfect ductile. The stress fields derived for the step area predict that fault patterns, mode of deformation and vertical displacement are different for the two rheologies. These predictions are illustrated for basins and swells developed in laboratory experiments with modelling materials.

The structure of basins and swells along the Dead Sea transform is discussed here. The pull-apart basins display an intensively faulted southern end and a gently dipping flexure at the northern end. A consistent dissimilarity appears between the structures of the eastern and western boundary faults of the basins. According to the present interpretation, these dissimilarities reflect a relatively ductile crust in Arabia and a relatively brittle crust in Sinai-Israel.

Introduction

Pull-apart basins and push-up swells are local zones of depression and uplift along strike-slip faults. Their development is attributed to the geometry of the faults: basins and swells form where strike-slip faults are bent, discontinuous or stepped (Fig. 1). The models of pull apart basins and push-up swells predict fault patterns as well as the relations between the amount of displacement and the dimensions of structures (Fig. 1). The present study examines how these predictions depend on the mechanical properties of the crust, and applies the results to the crust along the Dead Sea transform.

Trevisan (1939) was probably the first to propose that the displacement along two wrench faults, which are stepped with respect to each other, generates local folding and thrusting. He

presented his model as an explanation for the Brenta Mountains in the Lombardy Alps. In recent terminology the Brenta Mountains would be considered a push-up swell or a pressure ridge (for terminology see Mann et al., 1983). Quennell (1956), proposed that the Dead Sea is a void in the crust caused by the overlapping segments of the Dead Sea fault system. Quennell was probably the first to recognize the pull-apart basin or rhomb-shaped graben. The concept of pull-apart basins was formulated later by Burchfiel and Stewart (1966) for the Death Valley, California, by Freund (1965) for the Dead Sea area, and many others (Aydin and Nur, 1982; Mann et al., 1983).

Here, the predicted stress distribution at the proximity of two faults in en-echelon pattern is presented for two idealized rheologies, brittle and ductile. Then, the pull-apart basins (PAB) and push-up swells (PUS) that form in a series of

laboratory experiments with wet clay and window putty are displayed. And finally, the structure of some basins and swells along the Dead Sea transform is described, and the corresponding crustal rheology is discussed.

Models for pull-apart basins and push-up swells

Pull-apart basins and push-up swells are zones of subsidence and uplift, respectively, in a strike-slip region. While the shape and dimensions of the PAB or the PUS may resemble the shape and dimensions of basins and swells of other environments, their development is linked to the patterns of the master strike-slip faults and the crustal rheology. Therefore, the following account emphasizes the fault pattern and the rheology, even though the dominant topographic features may be the basins and the swells.

The simplest model of a pull-apart basin includes two parallel strike-slip faults that are slightly stepped with respect to each other (Fig. 1). After a relatively small slip along the faults they are connected by at least one cross fault at the step, dividing the region into two blocks separated by a stepped fault zone. Additional slip along the strike-slip faults will open a hole in the step area.

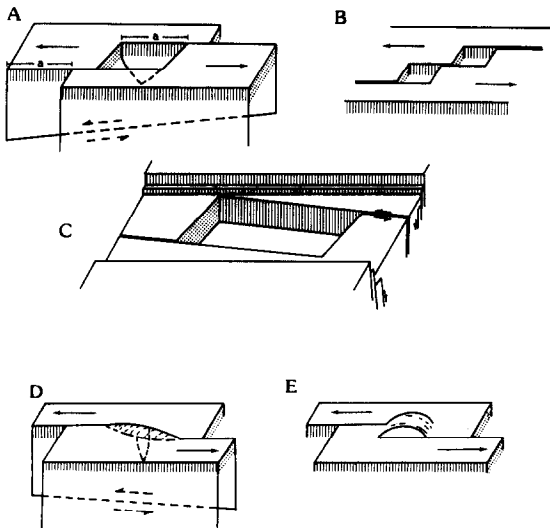


Fig. 1. Idealized models of pull-apart basins, in A, B and C, and of push-up swells, D and E. Note coalescing faults in the subsurface of A and D. Slightly modified after Garfunkel (1981).

This hole is the pull-apart basin. Following Sibson (1985), *dilational jog* is a right step along a right-lateral fault, or a left step along a left-lateral fault (Fig. 1A) and an *anti dilational jog* is a right step along a left lateral fault, or a left step along a right-lateral one (Fig. 1D). A dilational jog generates a pull-apart basin, whereas an anti dilational jog generates a push-up swell (Fig. 1E).

This model and its modifications (Garfunkel, 1981; Aydin and Nur, 1982; Mann et al., 1983) are based, explicitly or implicitly, on the following assumptions: (1) The volume of the crust is constant during the strike-slip displacement; this is sometimes simplified to assume constant area (Figs. 1A, B). (2) The deviation of the slip direction from the strike of the fault should yield vertical displacement, with associated horizontal extension or horizontal compression. The most conspicuous vertical displacement occurs at the step, as this is the location of the largest deviation between the slip direction and the fault strike. (3) The crust behaves as a brittle-elastic material (note the rigid blocks in Fig. 1). The third assumption is probably a simplified one; however, it has some significant implications on the model predictions, as shown below.

Segall and Pollard (1980) and Rodgers (1980) were the first to analyze the elastic stress field in the vicinity of a step. They used different approaches: Segall and Pollard analyzed the interaction between the two faults, whereas Rodgers calculated the superposition of the contributions of the faults. Their results are generally similar: The mean stress, $\frac{1}{2}(\sigma_1 + \sigma_3)$, decreases *inside* the step between the faults for a dilational jog (Fig. 2a) and decreases *outside* the step of an anti dilational jog (Fig. 2c). The maximum shear stress, $\frac{1}{2}(\sigma_1 - \sigma_3)$, behaves differently. For a dilational jog the maximum shear stresses increase at fault ends with a slight larger increase *outside* the step (see contours in Fig. 2b). For the anti dilational jog the maximum shear stresses increase *inside* the step (Fig. 2d). These modifications of the stress fields at the step area should affect the style by which the initial faults coalesce in different rheologies.

Consider the geometry of PAB and PUS that develops in two idealized rheologies, brittle and

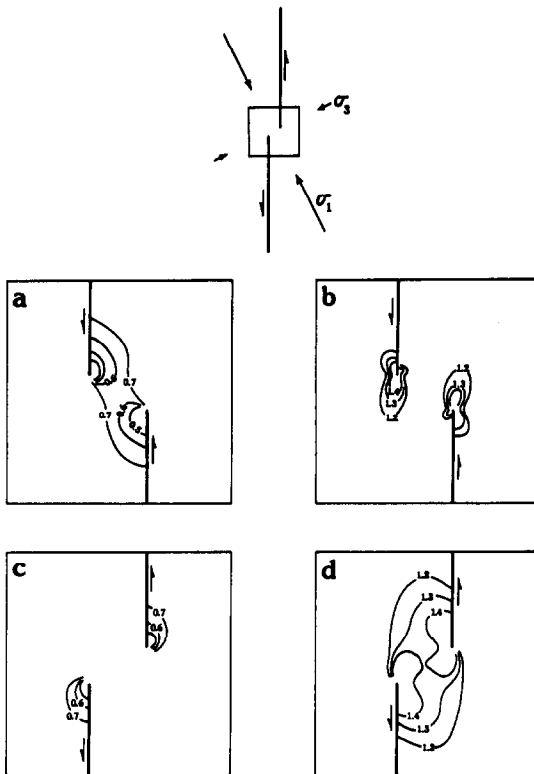


Fig. 2. The local stress field near a step between two left-lateral faults due to slip along the faults. Upper diagram indicates general geometry; σ_1 and σ_3 are maximum and minimum compressive stresses, respectively; details within the marked square are shown below. The marked values of shear and mean stresses are with respect to the far-field value of 1; thus values smaller than unit 1 indicate stress reduction and values larger than unit 1 indicate stress increase. a. Contours of the reduced mean stress, $\frac{1}{2}(\sigma_1 + \sigma_3)$, near a dilational jog. b. Contours of increased shear stresses, $\frac{1}{2}(\sigma_1 - \sigma_3)$, near a dilational jog. c. Contours of reduced mean stress near anti dilational jog. d. Contours of increased shear stresses near anti dilational jog. (After Segall and Pollard, 1980.)

ductile. Brittle rheology here means a material that tends to yield by extension fracturing; a material in which the yielding strength depends primarily on the magnitude of the mean stress; and a material that usually develops discreet, narrow faults. Frequently a brittle material is associated with frictional strength according to "Byerlee's law" (Fig. 3a). Ductile rheology here means a material that tends to shear and flow and in which the yielding strength is independent of the mean stress (Fig. 3b). Shear faults form in this ductile material; however, the slip along these faults occurs by creep without stress drop and elastic en-

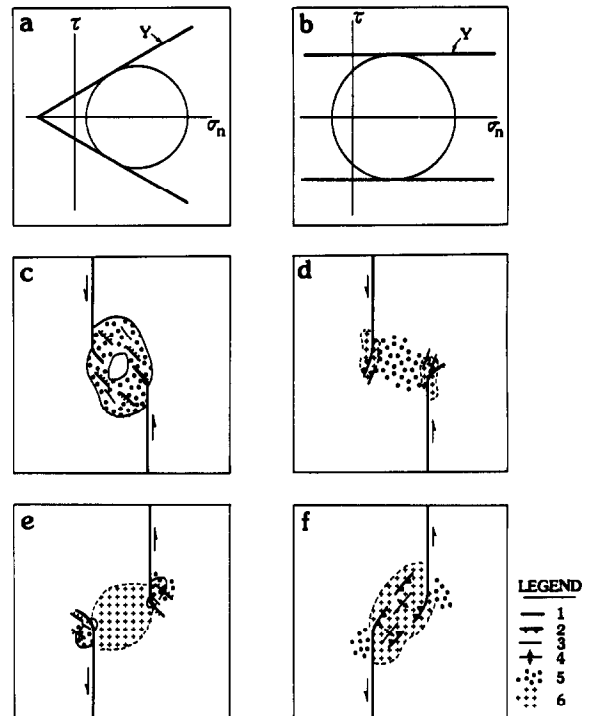


Fig. 3. Predicted structures at dilational and anti dilational jogs. a. Yield envelope of an idealized brittle material (Mohr diagram). b. Yield envelope of an idealized ductile material (Mohr diagram). c. and e. Predicted structure of a dilational jog (pull-apart) and an anti dilational jog (push-up), respectively, in a brittle material. d. and f. Predicted structure of a dilational jog (pull-apart) and an anti dilational jog (push-up), respectively, in a ductile material (see text). 1 = strike slip fault; 2 = reverse-strike-slip fault; 3 = normal-strike-slip fault; 4 = fold axis; 5 = subsidence area; 6 = uplifted area.

ergy release. The brittle material has low strength in tension, and thus, the reduction of the mean stress increases its tendency to yield (Fig. 3a). On the other hand, the ductile material maintains equal strength under tension or compression, and, thus, only an increase of the shear stresses increases its tendency to shear (Fig. 3b).

This difference in yielding behavior between the two rheologies produces a difference in the style of faulting in the step area. Faults in the brittle material should propagate into the regions of lower mean stresses. Thus, the initial faults should propagate *toward* one another in a dilational jog (Fig. 3c), whereas in an anti dilational jog the initial faults should propagate *away* from one another (Fig. 3e) (Segall and Pollard, 1980).

These predictions are supported by field evidence (Segall and Pollard, 1980) as well as laboratory results (Horii and Nemat-Nasser, 1985).

Faults in the ductile material should propagate into the regions of high maximum shear stresses. Thus, in a dilational jog the initial faults propagate *away* from each other (Fig. 3d) and in the anti dilational jog the faults propagate *toward* one another (Fig. 3f). Furthermore, the propagating sections of the faults are different for the two types of rheologies. In the brittle material, the propagating portions of the initial faults are mixed normal and strike-slip faults (Figs. 3c, e), whereas in the ductile material they are mixed reverse and strike-slip faults (Figs. 3d, f).

The zone between two faults arranged in a dilational jog is subjected to extension; the mode of yielding to this extension depends on the local crustal rheology. If one considers a brittle crust the two master strike slip faults would link by two extensional branches and a basin bounded by faults would develop (Figs. 1, 3c). This mode predicts that the length of the basin is equal to or larger than the amount of displacement along the master strike-slip faults (Fig. 1). The length of the basins can then be used to determine the minimum amount of slip (Garfunkel, 1981), or to distinguish between basins of different ages (Garfunkel et al., 1981).

However, if one considers a ductile crust, the displacement along the master faults may be accommodated by other mechanisms. For example, accommodation by continuous extension inside the basin (Fig. 3d) as well as by continuous compression of the crust outside the basin. There-

fore, the length and width of a basin in a ductile crust cannot be easily predicted as summarized in Fig. 3 and Table 1.

The development of pull-apart basins and push-up swells in experiments

The nucleation and growth of PAB and PUS in samples of wet clay and window putty are presented here. The structures initiated and grew as a result of interaction between faults that were either pre-cut into the samples or that formed spontaneously during the experiments. The samples were up to 57 mm thick and up to 210 × 210 mm in area. They were loaded laterally in a constant strain rate. No "basement" with pre-cut faults or stepped faults was used; thus, the observed basins and swells reflect the response of the sample material to the applied deformation. Details of the apparatus and the experimental conditions appear in Reches (1987). Figures 4–7 show portions of the surface of samples deformed under equal area conditions, by loading parallel to the picture plane. In all figures maximum compression is in a N–S direction.

Figure 4 displays a sample of window putty before and after deformation. Two pairs of faults, with a right step and with a left step, were cut into the sample prior to deformation. All four faults are left lateral with some extension perpendicular to them. A zone of intense minor faulting indicates the direction of propagation at the termination of the large fault. Figure 4A shows that the left fault of the left step pair (marked a) bends *away* from its counterpart; the right fault in this

TABLE 1

Relationship between crustal rheology and the structure of pull-apart basins and push-up swells

Property	Brittle rheology	Ductile rheology
Fault bending		
(1) pull-apart basins	Toward each other	Away from each other
(2) push-up swells	Away from each other	Toward each other
Type of faulting	Oblique-normal and strike-slip faults	Oblique-reverse and strike-slip faults
Length/slip relations	Length of basin is equal to or larger than total slip	Length of basin has no simple relation to slip
Extension parallel to		
pull-apart basins	Extension equal to total slip	Extension is smaller than total slip
Style of deformation	Faulting	Continuous deformation and faulting

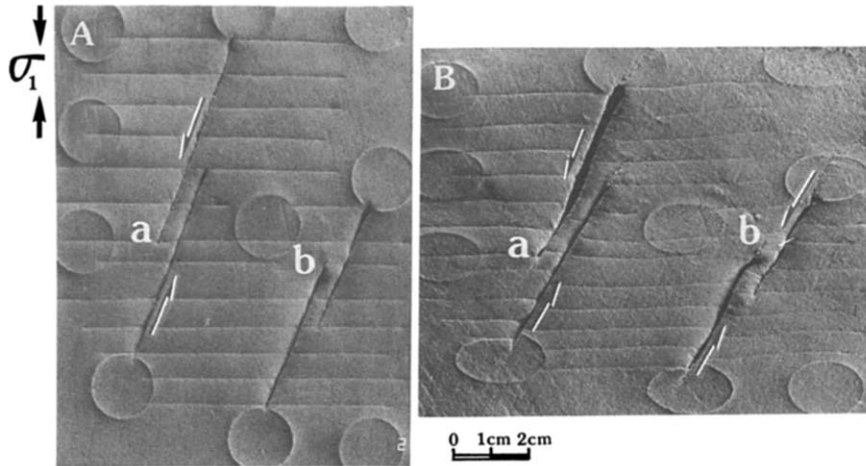


Fig. 4. Propagation of left-lateral faults in window putty. Maximum compression in N–S direction. A. Initial, precut faults. B. After 21% shortening; note the faults propagate toward each other at the left step and away from each other at the right step (see text).

pair bends only slightly. The left fault of the right step pair (marked *b*, Fig. 4B), bends *toward* its counterpart; the right fault in this pair did not bend. The zones inside the steps underwent extension in the left stepped pair and compression in the right stepped pair (Fig. 4B). The observed bending directions of faults *a* and *b* as well as the continuous deformation of the step zones, fit the predictions for a ductile material (Fig. 3d, f).

The development of a push-up swell in a wet

clay sample is shown in Fig. 5. Two large left-lateral faults with a left step, were precut into the sample (marked *a* and *b*, Fig. 5A). This configuration should have generated a PAB between *a* and *b*; however, these faults did not interact with each other, presumably due to the large spacing between them. Instead, fault *a* interacted with a new fault, *c*, which formed spontaneously at the southwest corner of the picture (Figs. 5B, C). The two interacting faults are connected by NE–SW

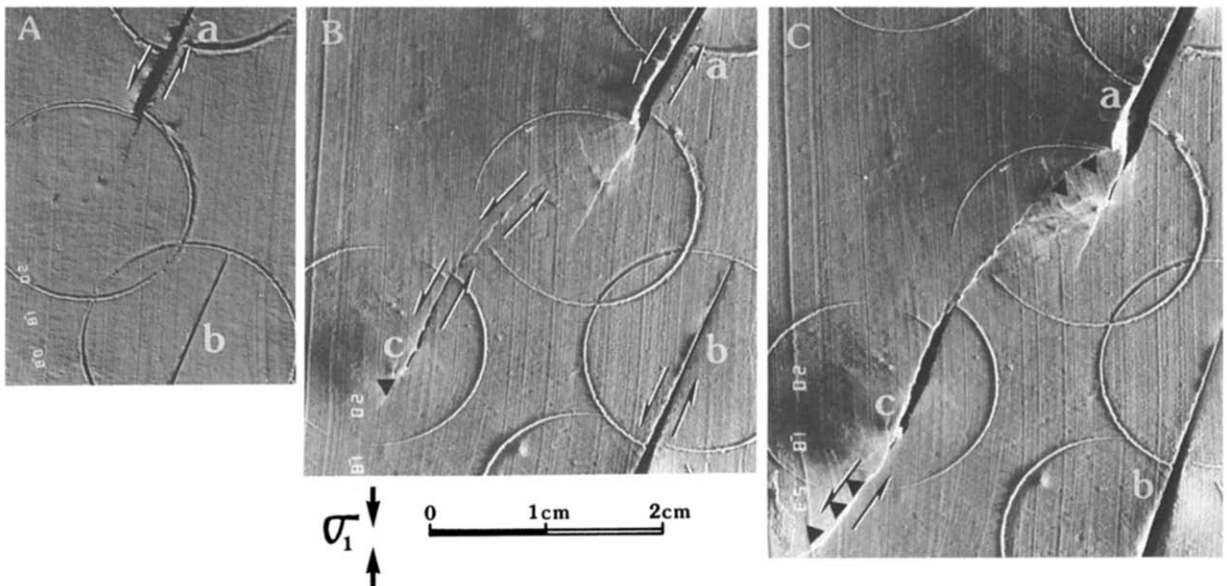


Fig. 5. Push-up swell development between left-lateral faults in wet clay. Maximum compression in N–S direction. Note initiation of PUS in B and lack of interaction between the two faults on the right side. Note in C the mixed reverse-strike-slip faults that bound the swell.

trending faults, which are oblique, strike-slip-reverse faults, and they enclose an uplifted area. The features that develop between faults *a* and *c* are in agreement with the predictions for an anti dilational jog in a ductile material (Fig. 3f).

According to the predictions in the section above, a shear fault in a brittle material should propagate into the region of the most reduced mean stress. Figure 6 tests this prediction for a single crack subjected to left lateral slip, precut into a hardened mixture of sand and gypsum powder (2.5%). Here, as in many other experi-

ments with brittle materials, the sample yielded unstably, and the fault extended as predicted (Horii and Nemat-Nasser, 1985).

The *spontaneous* development of pull-apart basins is rare in the present series of experiments. Figure 7 shows one case of a spontaneous PAB formed in a wet clay sample. The basin appears initially as an unfaulted topographic depression between two right-lateral faults (Fig. 7A). The depression is cut later by an extension fracture at its center (Fig. 7B). Afterwards, the PAB grows by two simultaneous mechanisms: the continuous

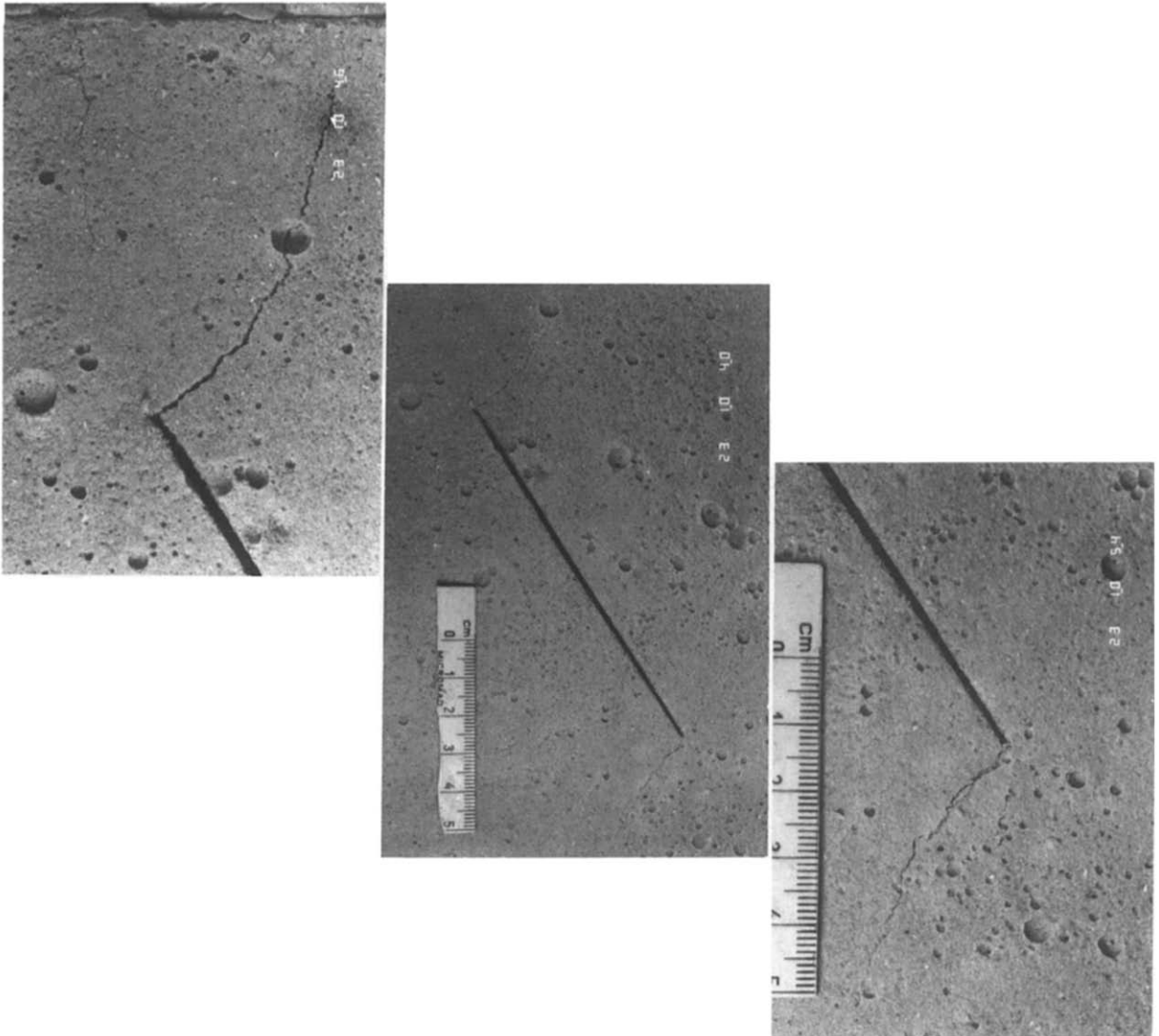


Fig. 6. Propagation of an open crack subjected to left lateral shear, in a brittle slab (sand cemented by 2.5% of gypsum powder). Maximum compression in N-S direction. Entire crack in center figure and details of both ends are in side figures.

subsidence of the depression and the opening of the extension fracture (Figs. 7C, D). As the deformation increases, the PAB lengthens, maintains its width and rotates together with its boundary faults (Figs. 7B, C, D). The PAB of Fig. 7 shows the modes of the two rheologies: continuous extension (ductile) and extension fracturing (brittle).

The experiments described above present some structures associated with PAB and PUS with their mechanical interpretation. These experiments are not models of field cases; rather, they are illustrations for the analysis proposed here.

Examination of basins and swells along the dead sea transform

The models of PAB and PUS which were presented above, provide a method of estimating the rheology of the crust in transform regions. This method is applied here to some of the better documented basins and swells along the Dead Sea transform.

The Dead Sea fault system is a leaky transform fault extending from the Red Sea to the Taurus Mountains between the Arabian plate and the Sinai-African subplate (Fig. 8) (Freund and Garfunkel, 1976; Garfunkel, 1981; Garfunkel et

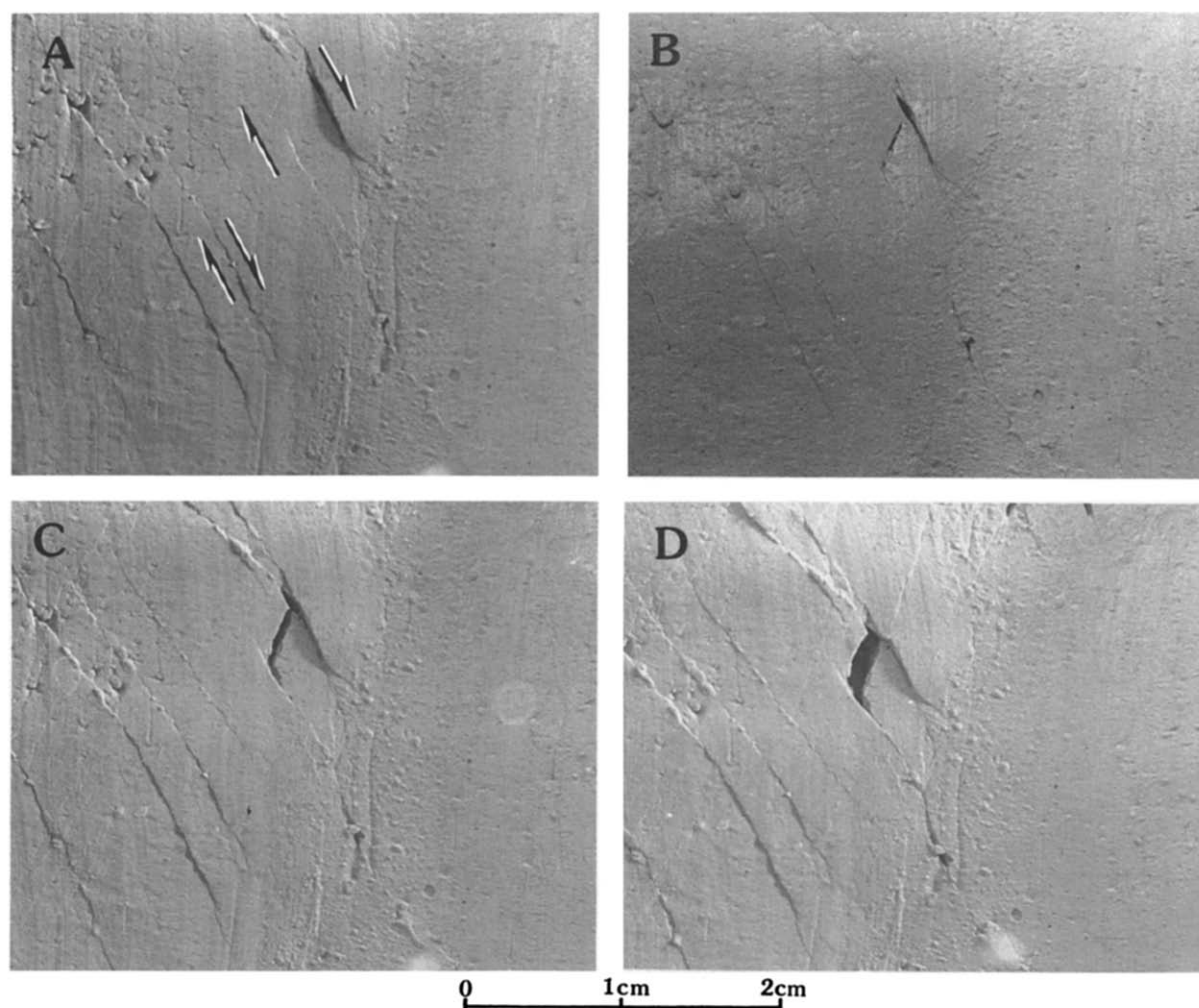


Fig. 7. Development of a pull-apart basin between right-lateral faults in wet clay. Note: in A, subsided area precedes the PAB; in B, connecting fault forms in lowest part of the subsidence; in C and D growth of the basin (see text).

al., 1981). The Dead Sea transform is discontinuous and includes more than ten PAB's and a few PUS's at its steps. The structural discussion below is based on the following characteristics: (a) Left-lateral displacement of about 105 km has occurred along the Dead Sea transform since the Middle Miocene (Freund and Garfunkel, 1976). (b) The stress field that exists along the transform can be represented by stresses determined from small

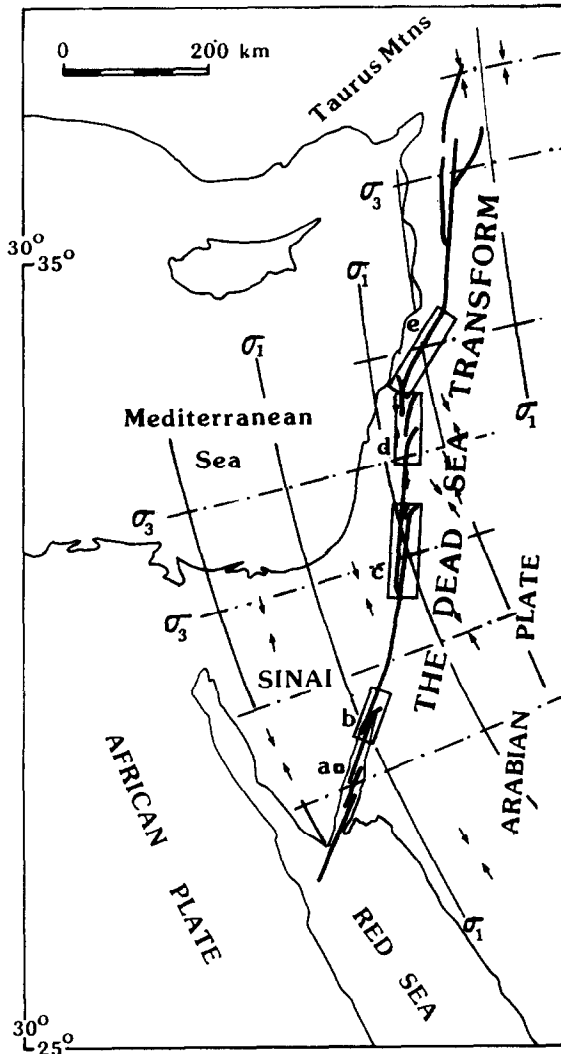


Fig. 8. General view of the Dead Sea transform. Strike-slip faults are marked in heavy lines; small arrows indicate maximum compression, and lines marked σ_1 and σ_3 indicate the directions of the maximum and minimum compressive stresses according to small scale structures (after Eyal and Reches, 1983); small frames along the transform indicate locations of Figs. 9-13.

scale structures by Eyal and Reches (1983) (Fig. 8). (c) The deformation along the Dead Sea transform is the result of dominant horizontal displacement parallel to the transform and minor extension normal to it.

The *Bir Zreir* graben in eastern Sinai is probably the best documented PAB anywhere (details in Eyal et al., 1985). The well exposed crystalline basement is crossed by several Miocene dikes, and thus, the fault traces and their displacements are accurately mapped (Fig. 9A). The *Bir Zreir* graben is bounded by fault systems on the west and the east. Both systems are longer than the graben and part of the displacement along them is not related to the formation of the graben. By omitting the displacements and the fault segments which seem unrelated to the graben, the simple map of Fig. 9B is produced. The extension along the line AA' (Fig. 9A) due to the three NW-SE trending faults (Fig. 9B) is calculated by Eyal et al. (1985) to be 1 km. This value is based on the measured dip of the northern fault and assumed dips of 60° for the other two faults. According to the model of a PAB in a brittle crust the extension along AA' (Fig. 9A) should be 2 km, equal to the strike-slip displacement along the eastern and western boundary faults (Fig. 1). Eyal et al. (1985) reject the PAB model because of this mismatch between calculated and predicted values of extension. They propose that the *Bir Zreir* graben was formed by a combination of left-lateral slip and block rotation.

According to the present study, however, the extension mismatch contradicts only a PAB model in a brittle crust, whereas in a partly ductile crust the apparent mismatch may be explained by the following mechanisms. The maximum subsidence in the *Bir Zreir* graben is about 1 km (Eyal et al., 1985) and thus, the graben is not a "hole" through the entire crust. It is likely therefore, that the western and eastern boundary faults coalesce at depth (Fig. 1A). Such coalescence reduces the amount of extension. Another mechanism to reduce extension *within* the graben, is shortening *outside* the graben, for example, shortening by reverse-strike slip motion along the diagonal fault that splays northeastward from the eastern fault, north of the graben (Fig. 9A). It is proposed therefore, that the *Bir Zreir* graben is a pull-apart

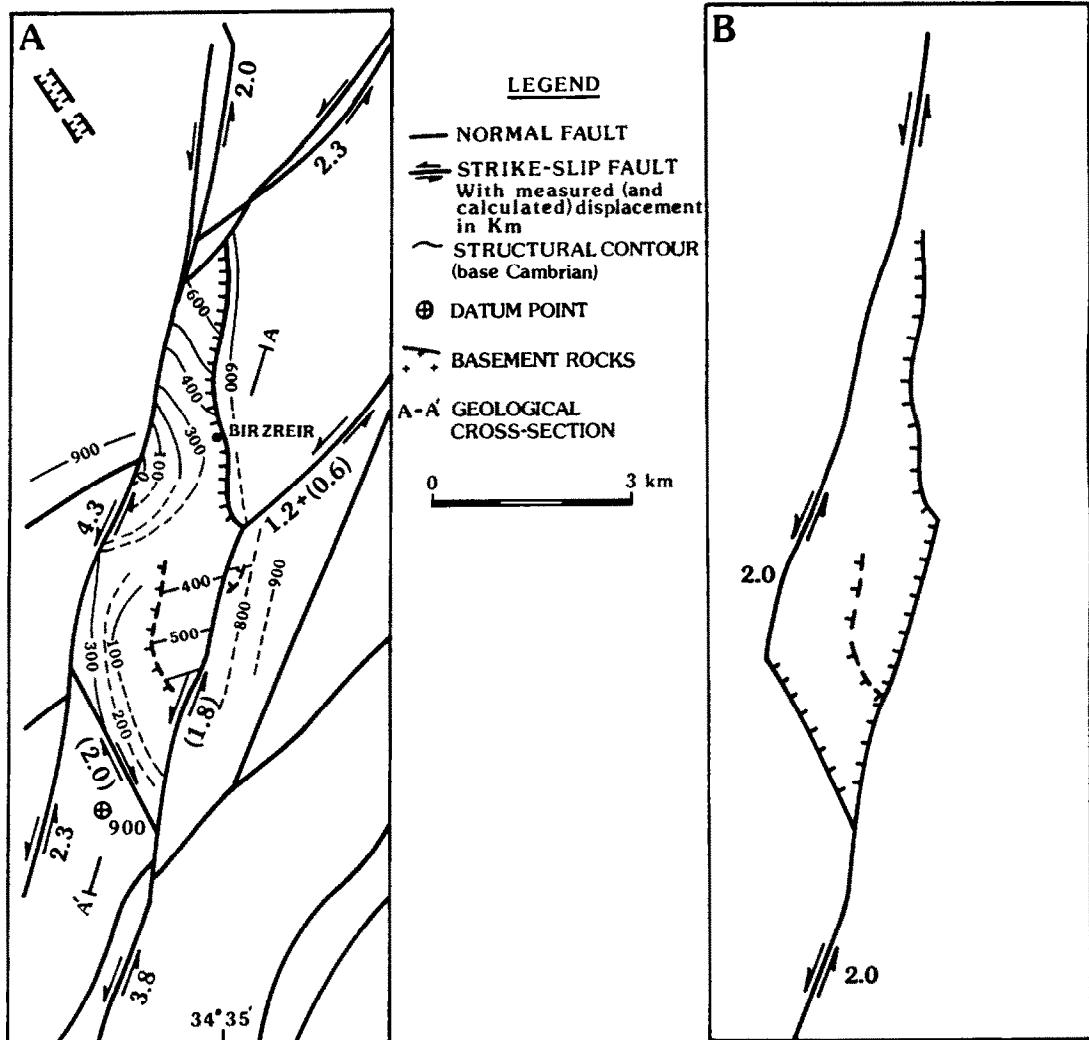


Fig. 9. Bir Zrier graben, eastern Sinai (location: frame *a* in Fig. 8). A. Structural map after Eyal et al. (1985). B. Simplified tectonic map produced by omitting faults and displacements unrelated to the pull-apart.

basin in partly ductile crust.

The *Elat Deep* studied by Ben-Avraham et al. (1979) is the northern basin of the Gulf of Elat. It is about 40 km long with a water depth of up to 900 m (Fig. 10). Both the western and eastern faults of this basin are dominated by vertical displacements (Ben-Avraham et al., 1979), whereas the southern fault appears as a strike slip fault (Ben-Avraham, 1985). The last observation does not fit the predictions of the PAB model of cross faults with normal slip (Fig. 1) (Ben-Avraham, 1985). Similarly to the position in Bir Zreir, faulting occurs only on the southern side of the Elat

Deep and the northern boundary of this basin is not faulted (Ben-Avraham et al., 1979); most likely it forms a southward dipping flexure. The western fault of the Elat Deep continues northward as the Elat fault (Fig. 10) (Reches et al., 1987). The Elat fault displays a continuous bend that forms the southern boundary of a new, small PAB. The direction of bending of the Elat fault is consistent with the predicted direction for the brittle crust (Fig. 3c). However, the eastern fault of the Elat Deep bends differently; it continues northeastward, *away* from the transform zone (Fig. 10). This new bending direction is typical north of the

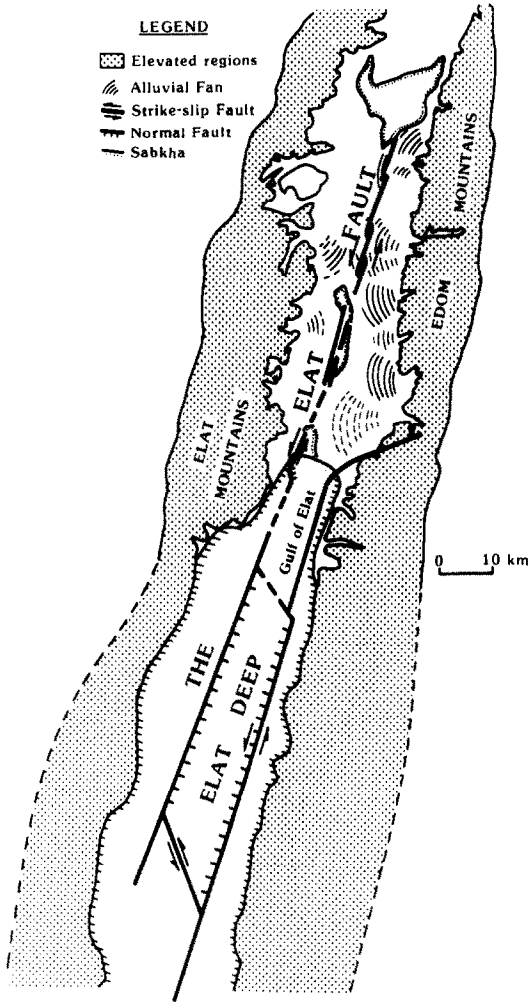


Fig. 10. The Elat Deep and the Elat fault (location: frame *b* in Fig. 8). Note: sense of slip along the margins of the Elat Deep, the lack of E-W faulting at the northern end of the basin, the northeastward continuation of the eastern fault and the bend in the center of the Elat fault. After Ben-Avraham (1985) and Reches et al. (1986).

Dead Sea, as described below.

The *Dead Sea* itself is the largest and most studied pull-apart basin in this transform system (Quennell, 1956; Freund, 1965; Neev and Hall, 1979; Garfunkel et al., 1981). According to most interpreters since Quennell (1956), both the east and west sides of the Dead Sea basin are delineated by large, oblique strike slip faults, as well as many subparallel normal faults. Some details of the internal structure of the basin have been revealed recently by deep seismic data (Ginzburg et

al., 1979; Ginzburg and Kashai, 1981; Kashai and Crocker, 1984; Arbenz, 1984). These studies indicate that the basin is bounded on the south by a few large listric faults, dipping toward the northeast, and on the north by a gentle flexure, dipping to the south (Fig. 11A, B). The large faults at the south are associated with many smaller faults of unclear pattern (Ginzburg and Kashai, 1981). Arbenz (1984) proposed that a large detachment surface extending from the listric faults under the entire Dead Sea basin (Fig. 11B). Garfunkel (1981) calculated 35 to 40 km of extension along the Dead Sea basin; he attributed this extension to the young slip phase, of Pliocene to Recent age. No PAB which is associated with the older phase (60–65 km slip), has been recognized at the proximity of the Dead Sea basin. Thus, Garfunkel (1981) proposed that either the older PAB's were obliterated during the young phase or that the plates motion during the old phase was parallel to

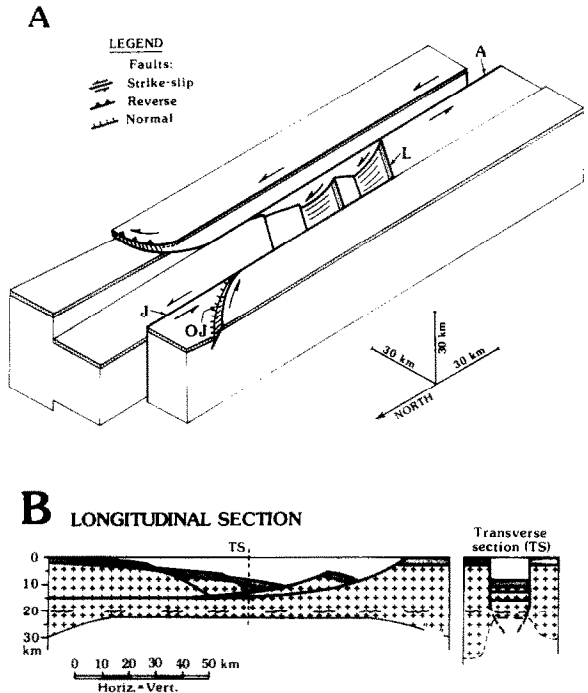


Fig. 11. Schematic presentation of the structure of the Dead Sea basin (location: frame *c* in Fig. 8). Modified after Arbenz (1984). A. Block diagram, *L*—listric faults at the south end; *A*—Arava fault; *J*—Jordan Valley fault; *OJ*—Aoj'a fault system. B. Cross sections. Note crustal thickness difference between east and west.

the Dead Sea transform without extension normal to it.

However, the extension within the Dead Sea basin may be only a portion of the whole deformation. As mentioned above, compression and thickening of the bounding plates *outside* the basin (Fig. 3d) are equivalent to extension *inside* the basin. For example, the thickening of Arabia implies less northward displacement of this plate, and the reduction of the total extension required for the Dead Sea basin. Indeed, recent seismic refraction profiles in Trans-Jordan indicate a crustal thickness of about 40 km along the dead Sea transform (Makris, 1985). On the western side of the transform, from north of Elat to north of the Dead Sea, the crustal thickness is 30 km or less (Ginzburg et al., 1979; Ginzburg et al., 1981). As the thinner western crust extends more than 100 km south of the Dead Sea, the greater thickness of the eastern side cannot be explained by a rigid displacement of 105 km of the Arabian plate. The thickening of Arabia and the accompanying isostatic compensation are consistent with the elevation difference between the two sides of the Dead Sea transform (see Discussion).

It is speculated here that the crust of the Arabian plate became thicker as the result of continuous ductile deformation. This suggestion agrees with the bending of the Arava fault to the northeast, propagating into the Arabian plate (Fig. 11A); this bending direction fits a ductile rheology (Fig. 3d).

A new zone of normal faults, the Aog'a system, appears northwest of the Dead Sea (Fig. 11A). This zone seems to splay gradually from the marginal faults of the rift: its trend varies from about N-S close to the rift to about NW-SE away from it. Similar zones occur along the western side of the rift from the Dead Sea to the Hermon.

In the east the thickening of the crust and bending of the Arava fault suggest a ductile rheology; within the transform zone the listric faults in the south and the flexure in the north indicate mixed rheology; and in the west the normal northwest fault system reflects a more brittle rheology. These differences in rheology indicators from one side of the transform to the other become even more

conspicuous north of the Dead Sea.

The three larger PAB's in the northern Jordan Valley (Fig. 12)—the Sea of Galilee, Hula and Ayun—display common structural features. The large strike slip faults that bound the basins are bent toward the northeast at their northern portions (Garfunkel et al., 1981; Garfunkel, 1981; Kashai and Crocker, 1985; Hieman and Ron, 1987). Many smaller NE-trending bends occur along some of these large strike-slip faults (Hieman and Ron, 1987) (Fig. 12b). Local uplifts bounded by curved, oblique reverse faults are associated with these small bends. Most bends in this region are in the direction predicted for a ductile crust (Fig. 3d, f). The surface features and the limited subsurface data (Kashai and Crocker, 1985), do not indicate large normal faults at either the northern or the southern boundaries of the three basins. The layers at these boundaries are most likely flexed into the basins, similarly to the flexures in the northern parts of the Bir Zreir graben (Fig. 9), the Elat deep (Fig. 10) and the Dead Sea basin (Fig. 11).

A few systems of prominent normal faults, which trend from NWW-SSE to almost W-E, are developed along the margins of the northern Jordan Valley (Fig. 12). These faults form a series of large blocks, usually tilted to the southwest. If these systems, as well as the Aog'a system mentioned above, are related to the left-lateral slip along the Dead Sea transform, then they indicate extensional yielding in the zone of reduced mean stresses (see model presentation above); such yielding fits brittle behavior of the crust. Thus, the west side of the transform in the north seems to behave more brittly than its east side, similarly to the above deduction about the Dead Sea area.

The *Hermon and Buruk Mountains*, farther north, form a huge push-up swell along a right step of the Dead Sea transform (Fig. 12). The internal structure of these mountains is complex. However, the main strike-slip faults display a relatively simple pattern: the Yammuneh fault, which connects through this step, as well as the Rachaya and Roum faults, all bend towards the northeast at their northern parts (Fig. 12). Reverse slip is likely to occur along these faults, but there is no direct field evidence to support or reject this possibility.

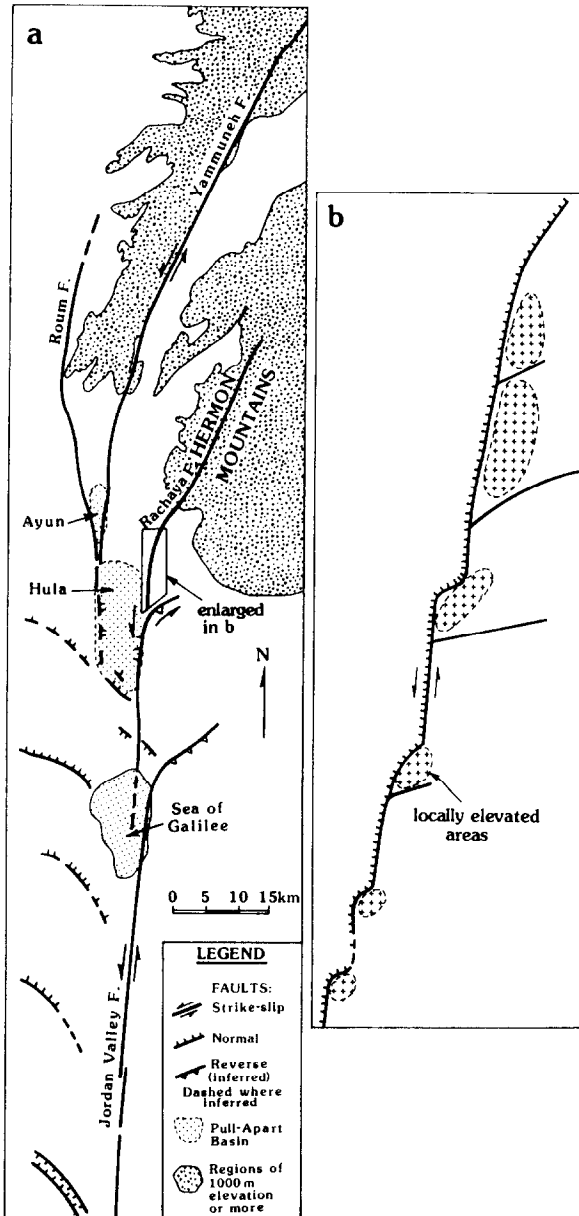


Fig. 12. a. Simplified tectonic map of northern Jordan Valley-Hermon Mountains (location: frames *d* and *e* in Fig. 8). After Garfunkel (1981) and Garfunkel et al. (1981). b. Details of the southern part of Rachaya fault. After Hieman and Ron (1986).

Discussion

In the description of the models for pull-apart basins and push-up swells, the effects of the crustal rheology on the geometry and nature of the domi-

nant strike-slip faults are presented (Fig. 3 and Table 1). The various geometries in a series of basins and swells were demonstrated in laboratory experiments with wet clay and window putty (Figs. 4–7). The geometry of a few major basins and swells in the Dead Sea transform was examined, and a consistent structural dissimilarity appeared between the west and east sides of the transform. According to the model presented here, the Arabian plate on the east is more ductile than the Sinai-Israel subplate on the west. The structural difference and the corresponding rheology difference, are recognizable from the Elat deep in the south to the Yammuneh fault in the north. This includes a segment of the transform almost 600 km long (Fig. 13).

It is proposed here that the apparent contrasting rheology reflects a difference in the heat conditions: the Arabian plate is warmer than the Sinai-Israel subplate. The crustal heat regime and the corresponding strength of the lithosphere have not been derived for the region of the Dead Sea transform; thus, only general indications may be considered. One expression of the proposed heat contrast is the marked difference in the abundance of young volcanic rocks. The Arabian plate includes a much larger distribution of volcanic fields of Miocene age or younger than the Sinai-Israel subplate (Fig. 13). Particularly conspicuous is the large volcanic field of the Gebel Druz region in southern Syria and northern Jordan (Fig. 13), as well as many smaller fields north and south of it. This idea is supported by the observation that in the northern Jordan Valley (Fig. 12a, b), both the eastern and western boundary faults are bent according to a ductile rheology (maps in Hieman and Ron, 1987). As igneous fields appear on both sides of the transform as well as within it in the northern Jordan Valley (unlike the southern part, Fig. 13), it is speculated here that the occurrence of the young igneous rocks around the Dead Sea transform is an indicator of crustal ductility.

The topographic features along the Dead Sea system also seem to be in accordance with the proposed rheology. An elevation difference of 200 to 400 m exists between Arabia and Sinai-Israel (Figs. 13). If this region is in isostatic equilibrium, than such an elevation difference reflects varia-

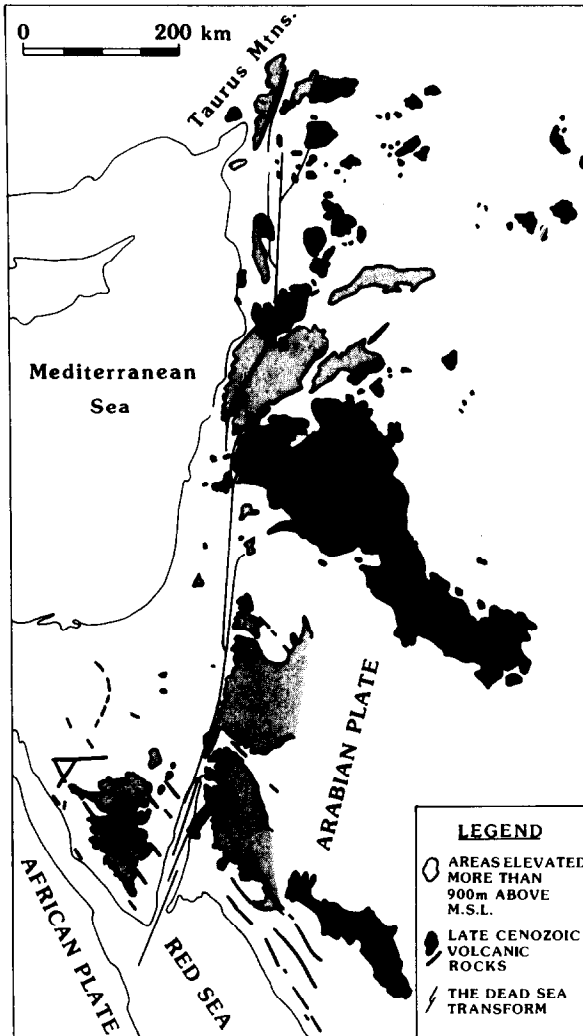


Fig. 13. Distribution of Cenozoic volcanic rocks and elevated areas in the region of the Dead Sea transform. After D. Mor (unpublished map).

tions in the density of the lithosphere, or, more likely, a difference in the thickness of the crust. For reasonable values of crustal and mantle densities, this elevation difference represents an Arabian crust thicker by 1.2 to 2.4 km than the Sinai-Israel crust. Makris (1985), reported a crustal thickness in southern Trans-Jordan of 40 km, determined in seismic refraction profiles, versus the 30 km thickness of the Sinai-Israel crust (Ginzburg et al., 1979). The marked thickening probably results from the combined effects of crustal development prior to the Miocene and tectonic thickening since the Miocene. The first effect may have led to the

localization of the Dead Sea transform along the suture between two different crusts. The second effect could have caused the accommodation of part of the motion between Arabia and Sinai-Israel by internal shortening in Arabia. If, as is proposed here, Arabia is more ductile than Sinai-Israel, then the greater tectonic thickening indeed occurs in the more ductile plate.

Conclusions

The main conclusions of the present study about the mechanics of pull-apart basins and about the Dead Sea transform are as follows: (1) The basic model of PAB and PUS (Fig. 1), is valid for a perfectly brittle-rigid crust. (2) The development of PAB and PUS in ductile crust forms fault patterns and length/displacement relationships that differ from their equivalents in the brittle crust, as summarized in Table 1 and Fig. 3. (3) The above conclusions provide a tool to estimate the overall rheology of the crust in transform zones. For the Dead Sea transform, it is found that the eastern Arabian plate is more ductile than the western Sinai-Israel subplate. This dissimilarity occurs along a segment of at least 600 km length.

Acknowledgements

Discussions with Zvi Garfunkel, David D. Pollard, Atilla Aydin, Paul Segall, Samuel Yoffe and Hagai Ron contributed significantly to the present work. Thanks are due to Doron Mor for the permission to use an unpublished map of his. The comments and reviews of Zvi Garfunkel, Atilla Aydin and Samuel Yoffe were constructive. The assistance of Sue Silkirk and Sally Larimer are appreciated. A special research grant from the Hebrew University supported this research.

References

- Arbenz, J.K., 1984. Oil potential of the Dead Sea area. Tel Aviv, Seismica, Rep. 84/111, 54 pp.
- Aydin, A. and Nur, A., 1982. Evolving of pull-apart basins and their scale independence. *Tectonics*, 1: 91-105.
- Ben-Avraham, Z., 1985. Structural framework of the Gulf of Elat (Aqaba), northern Red Sea. *J. Geophys. Res.*, 90: 703-727.

- Ben-Avraham, Z., Almagor, G. and Garfunkel, Z., 1979. Sediments and structure of the Gulf of Elat. *Sediment. Geol.*, 23: 239–267.
- Burchfield, B.C. and Stewart, J.H., 1966. "Pull apart" origin of the central segment of Death Valley, California. *Geol. Soc. Am. Bull.*, 77: 439–442.
- Eyal, Y. and Reches, Z. 1983. Tectonic analysis of the Dead Sea rift region since the Late-Cretaceous based on mesostructures. *Tectonics*, 2: 167–185.
- Eyal, Y., Eyal, M., Bartov, Y., Steinitz, G. and Folkman, Y., 1985. The origin of the Bir Zreir rhomb-shaped graben, eastern Sinai. *Tectonics*, in press.
- Freund, R., 1965. A model of the structural development of Israel and adjacent areas since Upper Cretaceous times. *Geol. Mag.*, 102: 189–205.
- Freund, R. and Garfunkel, Z. 1976. Guidebook to the Dead Sea rift. *Dep. Geol., Hebrew Univ., Jerusalem*, 27 pp.
- Garfunkel, Z., 1981. Internal structure of the Dead Sea leaky transform (rift) in relation to plate kinematics. *Tectonophysics*, 80: 81–108.
- Garfunkel, Z., Zak, I. and Freund R., 1981. Active faulting along the Dead Sea transform (rift). *Tectonophysics*, 80: 1–26.
- Ginzburg, A. and Kashai, E., 1981. Seismic measurements in the southern Dead Sea. *Tectonophysics*, 80: 67–80.
- Ginzburg, A., Makris, J., Fuchs, K., Prodehl, C., Kaminski, W. and Amitai, U., 1979. A seismic study of the crust and upper mantle of the Jordan–Dead Sea rift and their transition toward the Mediterranean Sea. *J. Geophys. Res.*, 84: 1569–1582.
- Ginzburg, A., Makris, J., Fuchs, K. and Prodehl, C., 1981. The structure of the upper mantle in the Dead Sea rift. *Tectonophysics*, 80: 109–119.
- Heiman, A. and Ron, H., 1986. Young faults in the Hula pull-apart, central Dead Sea Transform. *Tectonophysics*, 141 (this issue): 117–124.
- Horii, H. and Nemat-Nasser, S., 1985. Compression-induced microcrack growth in brittle solids: axial splitting and shear failure. *J. Geophys. Res.*, 90: 3105–3125.
- Kashai, E. and Crocker, P.F., 1984. New evidence concerning the tectonics of the Dead Sea rift. *Israel Geol. Soc. Annu. Meet.*, 1984, Arad, pp. 54–55.
- Kashai, E. and Crocker, P.F., 1985. New evidence concerning the tectonics and sedimentation of the Bet Shean–Kinneret and the Hula grabens. In: *Int. Workshop Sedimentary Basins of the Dead Sea and Other Rift Zones*, Geophysics, Tel Aviv Univ.
- Makris, J., 1985. (Lecture given in *Int. Workshop Sedimentary Basins of the Dead Sea and other rift zones*, Geophysics, Tel Aviv Univ.
- Mann, P., Hempton, M.R., Bradley, D.C. and Burke, K. 1983. Development of pull-apart basins. *J. Geol.*, 91: 529–554.
- Neev, D. and Hall, J., 1979. Geophysical investigations in the Dead Sea. *Sediment. Geol.*, 23: 209–238.
- Quennell, A.M., 1956. Tectonics of the Dead Sea rift. *Int. Geol. Congr.*, 20th, Mexico—Assoc. Serv. Geol. Afr., pp. 385–405.
- Reches, Z., 1987. Evolution of fault patterns in clay experiments. *Tectonophysics*, in press.
- Reches, Z., Erez, Y. and Garfunkel, Z., 1986. Sedimentary and tectonic features in the northwestern head of the Gulf of Elat, Israel. *Tectonophysics*, 141 (this issue): 169–180.
- Rodgers, D.A., 1980. Analysis of pull-apart basin development produced by en-echelon strike-slip faults. In: P.E. Ballance and H.G. Reading (Editors), *Sedimentation in Oblique Slip Mobile Zones*. *Int. Assoc. Sedimentol., Spec. Publ.*, 4: 27–41.
- Segall, P. and Pollard, D.D., 1980. The mechanics of discontinuous faults. *J. Geophys. Res.*, 85: 4337–4350.
- Sibson, R.H., 1985. Stopping of earthquake ruptures at dilational fault jogs. *Nature*, 316: 248–251.
- Trevisan, L., 1939. Il Gruppo di Brenta. *Mem. Inst. Geol. Mineral. Univ. Padova*, 13: 1–128.